The use of high strength steel in bridge decks

Pierre Thomas Jacques Lorne

pierre.lorne@epfl.ch

Abstract

Composite bridges combining steel plates with a concrete slab deck have been widely used due to their economic, constructive and structural advantages. In parallel, High Strength Steels (HSS) have emerged; their use in composite bridge decks could become an interesting option.

Three designs are presented for a composite steel-concrete roadway bridge, based on the Eurocodes: the design A, with two welded I-section girders in S355 steel; the design B, with two welded I-section girders in S690 steel; and the design C, with girders in S690 steel using tubular profiles for the flanges. A comparative analysis of the benefits associated with the three solutions is carried out.

During the design of solutions B and C, it is verified that some rules of EC3-1-5 are very conservative; adaptations are suggested for the case of AAR. By using tubular flanges, it is also possible to consider the webs to be fixed and not simply supported, as considered in the design C.

The design B presents several advantages compared to the solution A. The weight of the girders reduces consequently; the use of HSS provides more reserve in resistance at ULS. However, problems related to local buckling of the plates in the section and fatigue become critical in the design.

The design C was implemented to try to solve stability and fatigue issues. With a steel weight in the deck similar to solution B, the reserve in resistance at ULS is also high and lateral stability improves greatly. However, the problems related to fatigue remain, and the execution of some constructive details becomes more complex.

Keywords: High strength steel, Composite steel-concrete deck, Tubular flanges, Plate buckling, Lateral-torsional buckling, Fatigue.

1. Introduction

Composite bridges combining steel plates with a concrete slab deck have been widely used due to their economic, constructive and structural advantages.

In parallel, High Strength Steels (HSS) have emerged; their use in the design of composite road bridges could become an interesting option, because of their high static yield strength, their low selfweight, their good weldability and their high ductility. However, the use of HSS in bridges leads to slender plate girder elements, which creates plate buckling and fatigue issues.

In this work, three solutions are presented for the design of a composite steel-concrete deck for a roadway bridge, based on the Eurocodes: the design A, with two welded I-section girders in S355 steel; the design B, with two welded I-section girders in S690 steel; and the design C, with girders in S690 steel using tubular profiles for the flanges. A comparative analysis of the benefits associated with the three solutions is carried out.

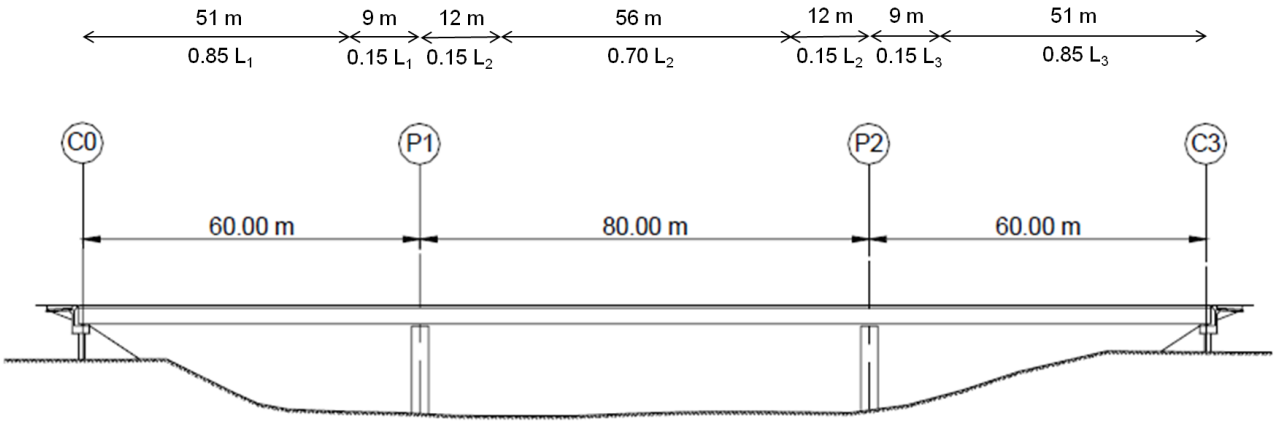

Figure 1: Longitudinal elevation of the bridge

2. Description of the bridge deck

2.1. Geometry

The critical cross-sections dimensions are presented in Table 1 and Figure 2.

Table 1: Dimensions of the steel girders

[mm]	Support P1			Mid-span P1-P2		
Design	A	B	C	A	B	C
$b_{f,sup}$ / D_f	1 000	650	457	1 000	650	457
$t_{f,sup}$	120	50	30	40	35	17.5
h_w	2 560	2 675	1 886	2 720	2 720	1 886
t_w	26	20	20	18	14	14
$b_{f,inf}$ / D_f	1 200	900	457	1 200	900	457
$t_{f,inf}$	120	75	40	40	45	36

The weight of the girders in the three solutions are compared in Table 2. The steel weight in solution B is 27% lighter than in solution A, which is a great improvement. The steel weight in the design C is 30% lighter than in solution A. Compared to the design B, the reduction of the steel weight is only 5%. Hence the design C is not a better solution than B regarding the weight of the girders.

Table 2: Comparison of the steel weights

	$g_{a,support,tot}$		$g_{a,span,tot}$		$g_{a,tot}$	
Design	A	B	A	B	A	B
A	0%	-	0%	-	0%	-
B	50%	0%	22%	0%	27%	0%
C	56%	13%	24%	2%	30%	5%

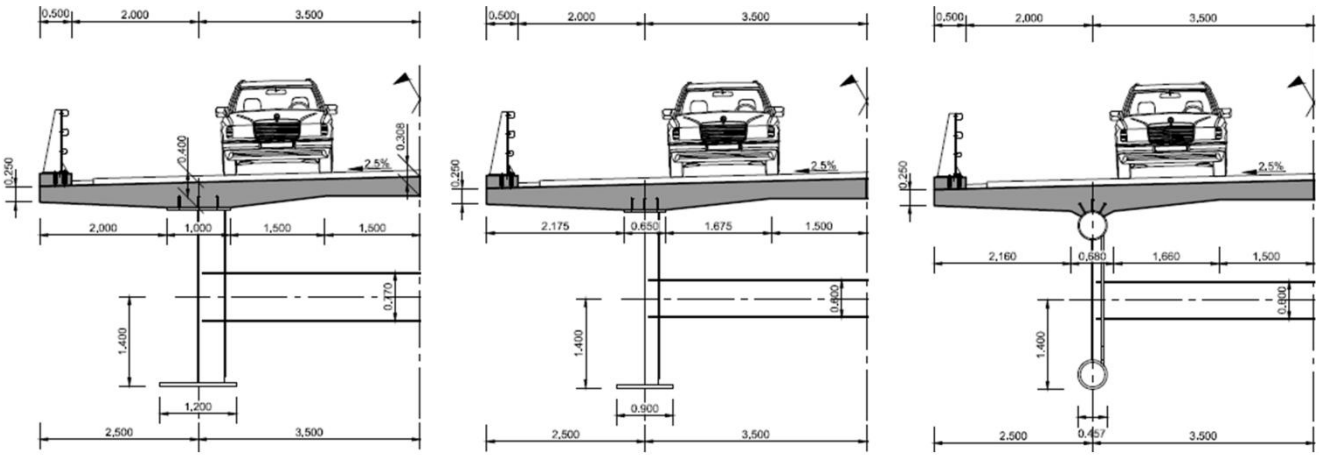

Figure 2: Left to right: solution A, B and C

2.2. Details

The details of the bracing frame and the vertical stiffeners are shown in Figure 3 and Figure 4.

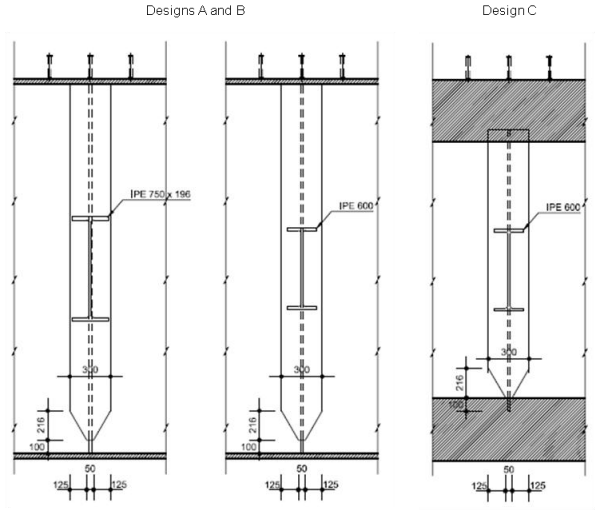

Figure 3: Cross-bracing frames

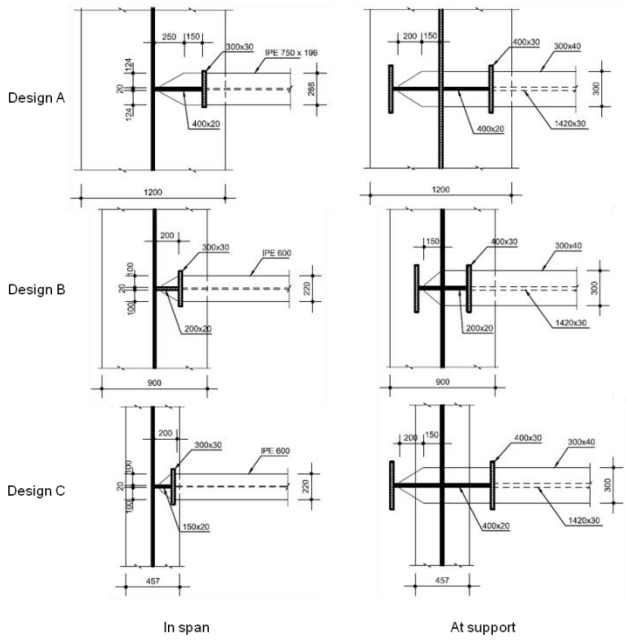

Figure 4: Transverse cross-section of the stiffeners

2.3. Cross-section classes

The elements of the girder can be classified into four classes [1], which determine if the cross-section can reach its plastic strength or its elastic resistance. Local buckling occurs in the class 4 elements before they reach their elastic resistance. The limit between classes 3 and 4 depends on the plate buckling coefficient k_σ, which depends on the stress ratio ψ in the girder. k_σ is given by equation (1) for $1 \geq \psi \geq 0$; (2) for $0 \geq \psi \geq -1$; and (3) for $-1 \geq \psi \geq -3$.

$$k_\sigma = \frac{8.2}{1.05 + \psi} \quad (1)$$

$$k_\sigma = 7.81 - 6.29 * \psi + 9.78 * \psi^2 \quad (2)$$

$$k_\sigma = 5.98 * (1 - \psi)^2 \quad (3)$$

The limiting slenderness of the web to draw the distinction between the cross-section classes 3 and 4 was then given by equation (4) for $1 \geq \psi \geq -1$ and (5) for $-1 \geq \psi$.

$$\frac{h_w}{t_w} \leq \frac{42 * \varepsilon}{0.67 + 0.33 * \psi} \quad (4)$$

$$\frac{h_w}{t_w} \leq \frac{124}{2} * \varepsilon * (1 - \psi) * \sqrt{-\psi} \quad (5)$$

In the EC3-1-1, the web is considered to be hinged to the plate flanges. However in the design C, the web can be assumed to be fixed to the tubular flanges. This new assumption is taken into account by the new formulas (6), (7) and (8), that have been developed to replace respectively the equations (1), (2) and (3).

$$k_\sigma = \frac{14.36}{1.06 + \psi} \quad (6)$$

$$k_\sigma = 13.54 - 6.29 * \psi + 19.69 * \psi^2 \quad (7)$$

$$k_\sigma = 9.88 * (1 - \psi)^2 \quad (8)$$

Hence the new limiting slenderness between the cross-section classes 3 and 4 is given by the formulas (9) and (10), which replace respectively the equations (4) and (5).

$$\frac{h_w}{t_w} \leq \bar{\lambda}_p \cdot \frac{1}{1.052} \cdot \sqrt{\frac{k_\sigma \cdot E_a}{235}} \cdot \varepsilon \quad (9)$$

$$\frac{h_w}{t_w} \leq \frac{156}{2} * \varepsilon * (1 - \psi) * \sqrt{-\psi} \quad (10)$$

The cross-section class depends on the stage of the bridge life. It is defined for all designs, at all critical cross-sections, in Table 3.

Table 3: Cross-section classes

	Support P1			Mid-span P1-P2		
Design	A	B	C	A	B	C
Construction	3	4	3	4	4	4
In service	3	4	4	1	4	3

At the final stage, the design A is in class 1 and can reach its plastic resistance. The design B is always in class 4, which implies that issues related to the local buckling of the web will appear. The design C is slightly better, thanks to the fixed connection between the web and the tubular flanges.

3. Global analysis and actions

Several actions are considered. The structural permanent loads include the selfweight of the girders and the concrete slab. The bridge equipment regroups the weight of the barriers and the asphalt layer. The variable actions are made of the temperature variations and the traffic actions, using the FLM1 at ULS and the FLM3 at ULS for fatigue. The effects of shrinkage are also considered.

The bridge is verified under two design combinations of actions [2]: the ULS and the ULS for fatigue.

The internal forces and moments are calculated with a model using the software SAP 2000, considering a first order and linear elastic analysis. The concrete is assumed to be cracked at supports, over a length equal to 15% of the span, on each side of the support, as shown in Figure 1. Hence the stiffness of the slab is equal to the stiffness of the reinforcing steel at supports.

The bridge is modelled as a continuous line of bar elements [3]. The girder is simply supported at piles and abutments. The reinforced concrete slab is modelled in the uncracked regions as a steel-equivalent area, with the modular ratios accounting for shrinkage ($n_s = 12$), long-term actions ($n_\varphi = 18$) and variable actions ($n_0 = 6$). The weights of the slab and the girders apply to the girders only.

4. Justification at ULS

4.1. Bending resistance

The verification of the bending resistance depends on the cross-section class.

At mid-span section in solution A is in class 1; hence it is checked with the plastic resistance moment $M_{pl,Rd}$ = 79.47 MNm, which is greater than the design bending moment M_{Ed} = 62.14 MNm.

All the other cross-sections and designs are in class 3 or 4. They are checked with the elastic resistance, using the effective cross-section when in class 4. The design stresses in the elements of the composite girder, and the design yield strength of the elements, are detailed in Table 4.

Table 4: Elastic bending justification

[MPa]	Support P1			Mid-span P1-P2		
Design	A	B	C	A	B	C
Class	3	4	4	1	4	3
$\sigma_{c,max}$	-	-	-	-10	-12	-13
f_{ck}/γ_c	-	-	-	-23	-23	-23
$\sigma_{s,moy}$	+152	+254	+283	-	-	-
f_{sk}/γ_s	+435	+435	+435	-	-	-
$\sigma_{y,sup}$	+269	+558	+676	-163	-316	-375
$f_{yk,sup}/\gamma_{M0}$	+295	+690	+690	-345	-690	-690
$\sigma_{y,inf}$	-253	-438	-671	+350	+467	+569
$f_{yk,inf}/\gamma_{M0}$	-295	-650	-690	+345	+690	+690

From solution A to solution B and then C, the stresses increase almost by a factor 1.7 and 1.8 in the reinforcing steel. In the concrete slab, the stresses do not vary much.

The working coefficient in the flanges at the extreme fibres is less in solutions B and C than in the design A. Hence compared to the design A, the solutions B and C provide more reserve in the resistance of the lower flange at ULS.

4.2. Shear resistance

The design shear resistance V_{Rd} is the minimum between the plastic design shear resistance of the web $V_{pl,a,Rd}$ and the design shear buckling resistance $V_{b,Rd}$ [4]. Only the participation of the web $V_{bw,Rd}$ is considered for $V_{b,Rd}$. It depends on the plate buckling coefficient for shear stresses k_τ:

$$k_\tau = 5.34 + 4/\alpha^2 \qquad (11)$$

The shear justification of the sections is detailed in Table 5.

Table 5: Shear justification

[MN]	Support P1			Mid-span P1-P2		
Design	A	B	C	A	B	C
$V_{b,Rd}$	8.13	8.86	7.39	4.45	4.30	3.95
$V_{pl,a,Rd}$	15.91	21.31	15.03	11.70	15.17	10.52
V_{Ed}	7.17	6.80	6.74	1.06	1.06	1.06

The calculations of the shear resistance in the Eurocodes come from the rotated stress field theory, which gives good results for web panels with high aspect ratios α [5]. It considers that the tension field can be anchored in the plate flanges.

In the design C, the behaviour of the tubular flanges under shear force is not well-known, and the tubes could fail under punching shear. Basler's

theory is used because it considers that the tension field in the web can only be anchored in the next web panel through the transverse stiffeners [6]. The behaviour of a web panel is decomposed into the pre-critical contribution V_{cr} and the post-critical contribution V_σ:

$$V_{cr} = h_w \cdot t_w \cdot \tau_{cr} \quad (12)$$

$$V_\sigma = h_w \cdot t_w \cdot \left(\frac{f_{y,w} - \sqrt{3} \cdot \tau_{cr}}{2 \cdot \sqrt{1 + \alpha^2}} \right) \quad (13)$$

Table 6: Design C, hinged connection

[MN]	Support P1		Mid-span P1-P2	
	EC3	Basler	EC3	Basler
V_{cr}	-	4.48	-	1.54
V_σ	-	2.89	-	2.46
V_{Rd}	7.39	7.37	3.95	4.00
V_{Ed}	6.74		1.06	

The Eurocode and Basler's theory give very close results for a hinged connection between the web and the flanges.

The shear resistance of the design C can be improved with more accurate assumptions. Equation (14) is valid when the web is assumed to be hinged to the plate flanges as in solutions A and B. In the design C, it is considered to be fixed to the tubular flanges. This leads to a new equation for k_τ :

$$k_\tau = 9.0 + 3.3/\alpha^2 \quad (14)$$

Table 7: Design C, fixed connection

[MN]	Support P1		Mid-span P1-P2	
	EC3	Basler	EC3	Basler
V_{cr}	-	7.39	-	2.54
V_σ	-	2.09	-	2.19
V_{Rd}	8.80	9.48	4.79	4.72
V_{Ed}	6.74		1.06	

The shear resistance increases due to the change of boundary condition between the web and the flanges. The difference between EC3-1-5 and Basler for a fixed connection can be explained by the fact that the formulas from the rotated stress field theory of EC3-1-5 were calibrated only for a hinged connection.

4.3. Bending and shear interaction

In case $V_{Ed} \geq 0.5 \cdot V_{Rd}$, the bending and shear interaction in the web should be considered. It happens at support P1 for all designs. The internal forces and moments considered for the verification should be taken at a distance $h_w/2$ from the support.

The interaction criterion is:

$$\overline{\eta}_1 = \frac{M_{Ed,\frac{h_w}{2}}}{M_{pl,Rd}} \geq \frac{M_{f,Rd}}{M_{pl,Rd}} \quad (15)$$

$$\overline{\eta}_3 = \frac{V_{Ed,\frac{h_w}{2}}}{V_{Rd}} \quad (16)$$

$$\overline{\eta}_1 + \left(1 - \frac{M_{f,Rd}}{M_{pl,Rd}}\right) \cdot \left(2 \cdot \overline{\eta}_3 - 1\right)^2 \geq 1 \quad (17)$$

The criterion is verified for all designs.

5. Justification of the stability

5.1. Flange induced buckling

A girder subjected to a bending moment results in a curvature ϕ and axial forces N_f in the flanges. Because of the curvature ϕ, the forces N_f induce deflection forces in the girder and thus a uniform compression stress σ_z in the web of the girder.

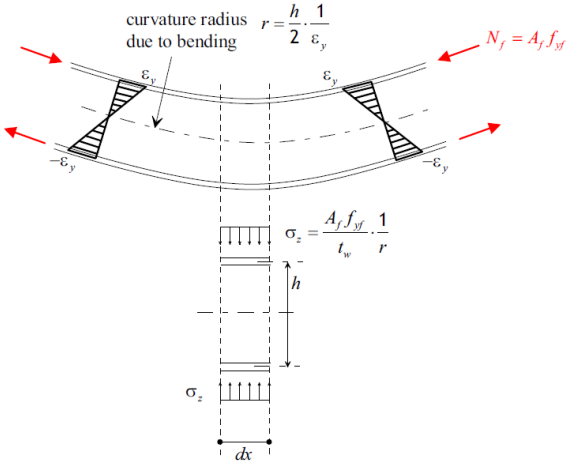

Figure 5: Flange induced buckling
[5] Figure 2.61

EC3-1-5 gives a criterion to avoid flange induced buckling:

$$\frac{h_w}{t_w} \leq k \cdot \frac{E}{f_{yk,inf}} \cdot \sqrt{\frac{A_w}{A_{f,inf}}} \quad (18)$$

This criterion is too conservative regarding the use of HSS. To account for the actual stress in the most used flange and the non-symmetry of the composite cross-section, the criterion becomes:

$$\frac{h_w}{t_w} \leq k \cdot \frac{E}{f_{yk,inf}} \cdot \sqrt{\frac{A_w}{A_{f,inf}}} \cdot \sqrt{\frac{h_i}{h_w} \cdot \frac{3}{m \cdot \left(m + \frac{1}{2}\right)}} \quad (19)$$

With m the ratio between the actual stress in the flange and the characteristic resistance of the flange.

The flange induced buckling is the limiting criterion for the thickness of the web of the girder. It can be reduced from solution A to solutions B and C, thanks to the use of HSS.

5.2. Lateral-torsional buckling

The compression flange must be justified against lateral-torsional buckling (LTB). The simplified check method is used for the verification.

The compression flange is assumed to be simply supported at piles and abutments. The bracing frame made by the cross-girders and the vertical stiffeners rigidify the cross-section. The resisting section is the effective area of the flange in compression and the effective part of the web near the flange. A distinction is made between the construction and the final stages of the bridge life.

At the construction stage, only the permanent structural actions apply: the weights of the structural steel girder and the concrete slab. The section is the upper flange at mid-span P1-P2 because it is in compression and not yet connected to the slab.

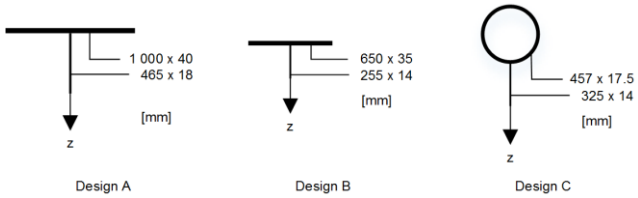

Figure 6: Compression upper flanges

During the construction of the bridge, the erection bracings are assumed to be rigid enough to provide a lateral support. The behaviour of the frame is shown in Figure 7.

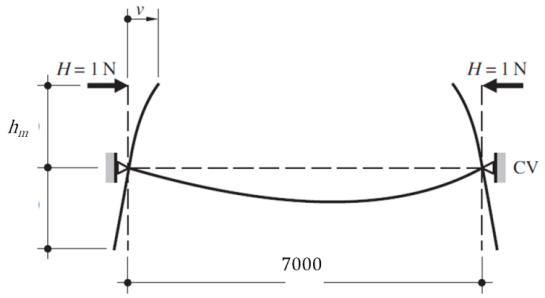

Figure 7: Bracing frame during the construction

At the final stage, all permanent and variable actions apply. The upper flange is connected to the slab and therefore is prevented from buckling. Hence the critical section is the lower flange at support P1.

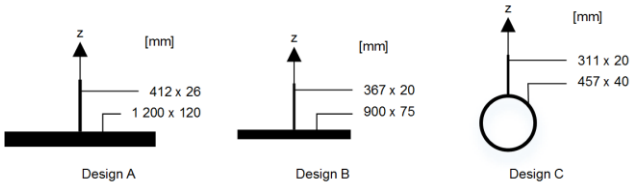

Figure 8 : Compression lower flanges

The cross-girders provide lateral elastic supports to the main girders. The behaviour of the frame is shown in Figure 9.

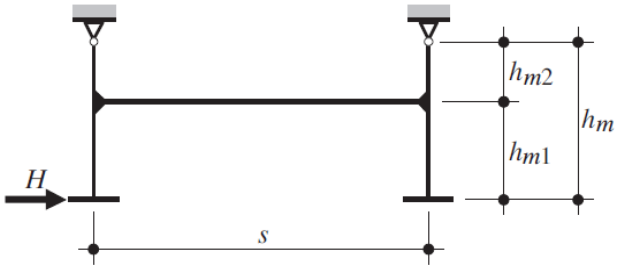

Figure 9: Bracing frame at the final stage

This model must be adapted in the case of tubular flanges, for the design C, as shown in Figure 10. It should be assessed with a model and tests.

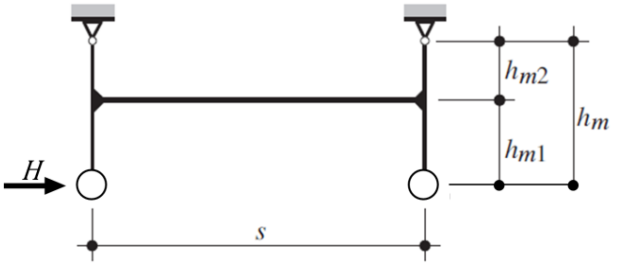

Figure 10: Bracing frame in the design C

Given the rigidity of the bracing frame, the critical axial load $N_{cr,D}$ can be calculated [7]. It is used to obtain the critical LTB stress $\sigma_{cr,D}$. The stress $\sigma_{cr,D}$ can be divided into the non-uniform and the uniform components σ_{Dw} and σ_{Dv}. The latter is neglected in designs A and B because the contribution of the flat flanges against torsion is small.

Then the design stress σ_{Ed} at the mid-plane of the flange should be less than the LTB stress σ_D. From EC3-1-1 [1], the buckling curve d for a welded I-section is used in the designs A and B; the curve a_0 for a hot finished hollow section is used in solution C.

The results are detailed in Table 8.

Table 8: Simplified check method

[MPa]	Support P1			Mid-span P1-P2		
Design	A	B	C	A	B	C
σ_{Dv}	0	0	1 989	0	0	2 206
σ_{Dw}	1 245	1 103	635	2 010	986	659
$\sigma_{cr,D}$	1 245	1 103	2 088	2 010	986	2 302
σ_{D}	211	354	586	263	350	590
σ_{Ed}	241	424	561	137	277	309

The design C provides more resistance against LTB than the other designs, thanks to the important contribution of the uniform component σ_{Dv} of the critical stress $\sigma_{cr,D}$.

There is no problem of stability of the upper flange during the construction. At the final stage, solutions A and B provide insufficient resistance against LTB of the lower flange.

The simplified method is conservative, considering a constant moment distribution along the bridge deck. More accurate calculations should be carried out.

The general check method consists in performing critical load calculations as exactly as possible. A model of a continuous simplified girder is modelled with an area made of the lower flange area and a sixth of the web. The rigidity of the bracing frame is accounted for as a spring at the bracing frame locations.

The analysis provides the minimum amplification factor $\alpha_{cr,op}$ to apply to the critical forces to reach the critical elastic resistance of the girder with regard to LTB. The reserve in elastic resistance at ULS in the lower flange is taken into account by the minimum amplification factor $\alpha_{ult,k}$ to apply to the design stresses to reach the characteristic resistance of the cross-section.

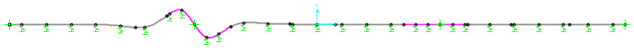

Figure 11: First buckling mode of failure

Several cases are considered:

a) The original cross-girders, made of IPE 600, are considered.
b) The bracing frames are strengthened by replacing the IPE 600 with IPE 750x196.
c) Only the two cross-girders around each support are strengthened by replacing the IPE 600 with IPE 750x196.

Table 9: General check method

	Design A			Design B		
Case	a)	b)	c)	a)	b)	c)
$\alpha_{cr,op}$	8.59	12.21	12.05	4.55	5.59	5.56
σ_{Ed}	241	241	241	424	424	424
$f_{yk,inf}$	295	295	295	690	690	690
$\alpha_{ult,k}$	1.22	1.22	1.22	1.53	1.53	1.53
χ_{op}	0.87	0.91	0.91	0.72	0.76	0.76
> 1 ?	0.963 < 1	1.013 > 1	1.011 > 1	1.008 > 1	1.062 > 1	1.061 > 1

In the design A, it is necessary to strengthen the two cross-girders around the support. In the design B, it is not required, though safer to strengthen these two cross-girders, as in the design A. It should be noticed that the difference between the cases b) and c) is very little.

With the general check method, the use of HSS is an advantage against LTB. Although the lower flange is slenderer in the solution B than A, the reserve in resistance represented by the factor $\alpha_{ult,k}$ provides more safety to the design B.

5.3. Stability of the cross-bracings

The shear resistance check and the LTB verification assume that the vertical stiffeners are prevented from torsional buckling. It should be justified in case of open stiffeners like flat or T-shaped stiffeners [5].

The general criterion neglects the warping stiffness of the transverse stiffener [8]:

$$\frac{G_a \cdot I_T}{I_p} \geq 2 \cdot f_{yk,T} \qquad (20)$$

When it is too conservative, the warping stiffness of the transverse stiffener can be taken into account:

$$\frac{1}{I_p} \cdot \left(\frac{\pi^2 \cdot E_a \cdot I_w}{{h_w}^2} + G_a \cdot I_T \right) \geq 6 \cdot f_{yk,T} \qquad (21)$$

The stiffeners are assumed to be fully loaded. It is too conservative in the case of HSS, where the actual stress can be taken into account:

$$\frac{1}{I_p} \cdot \left(\frac{\pi^2 \cdot E_a \cdot I_w}{{h_w}^2} + G_a \cdot I_T \right) \geq 6 \cdot \sigma_{act,Ed} \qquad (22)$$

The criterion from equation (22) is the only one to be fulfilled by all the designs.

6. Fatigue Safety Verification

6.1. Web breathing

Under cyclic loading due to the traffic actions, the initial out-of-plane imperfections can increase or decrease, and induce stress variations in the web, that produce damages due to fatigue in the welds between the web and the flanges of the girder.

Two different criteria account for the web breathing. EC3-2 limits the height of the web to a value that depends on the length L of the span:

$$\frac{h_w}{t_w} \leq \min\,(30 + 4 \cdot L; 300) \qquad (23)$$

This criterion is more critical for the side spans, which are smaller than the intermediate span. Another criterion, based on an empiric formula limits the compression height h_c of the web [6].

$$\frac{h_c}{t_w} \leq 100 \qquad (24)$$

The results are detailed in Table 10.

Table 10: Web breathing

	Support P1			Mid-span P1-P2		
Design	A	B	C	A	B	C
h_c/t_w	47.6	56.3	46.7	47.2	70.0	46.8
h_w/t_w	98.5	133.8	94.3	151.1	194.3	134.7
Limit	300	300	300	300	300	300

All cross-sections are verified.

6.2. Assessment of specific details

The FLM3 and the equivalent stress ranges simplified method (ESRSM) [4] can be used for fatigue calculations.

$$\gamma_{Ff} \cdot \Delta\sigma_{E,2} \leq \frac{\Delta\sigma_c}{\gamma_{Mf}} \qquad (25)$$

$$\Delta\sigma_{E,2} = \lambda \cdot \Phi \cdot \Delta\sigma_{fat} \qquad (26)$$

Important details are justified against fatigue: (1) the butt weld in the lower flange for the change in thickness; (2) the transverse weld of the vertical T-shaped stiffener web on the lower flange at mid-span P1-P2; (3) the butt weld of the lower flange to the vertical plate at support P1, in design C.

In equation (25), the safety factor for the strength of the detail γ_{Mf} is applied to the stress range $\Delta\sigma_{E,2}$; it is easier then to compare it with the FAT of the detail.

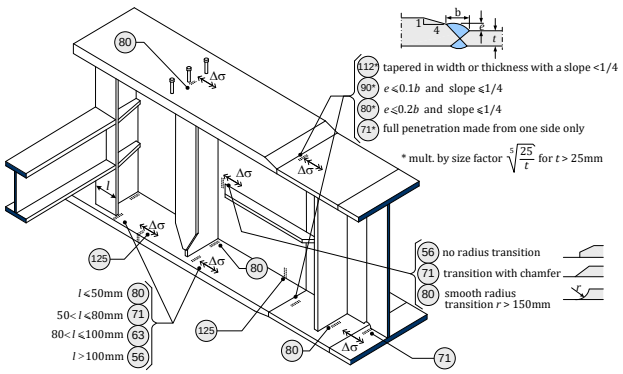

Figure 12: Typical FAT detail categories. Adapted from [3] Figure 9.10

The results are detailed in Table 11.

Table 11: Fatigue assessment [MPa]

Detail	1			2			3
Design	A	B	C	A	B	C	C
$\Delta\sigma_{fat}$	17.7	20.0	21.3	26.3	33.4	32,7	12.0
$\gamma_{Mf} \cdot \Delta\sigma_{E,2}$	41.0	46.5	49.4	61.1	77.5	75.9	31.6
$\Delta\sigma_c$	64.6	63.1	66.0	80.0	80.0	80.0	80.0

All the details are verified against fatigue. The detail of the transverse weld of the vertical T-shaped stiffener web on the lower flange at mid-span P1-P2 is the most critical. It has become decisive in the designs B and C, whereas it was not in the design A.

7. Conclusions

7.1. Analysis of the design B

Compared to the design A, the weight of the girders in the design B decreases consequently: The costs are reduced during the construction, thanks to the lighter deck and the economy of material.

The ULS is not critical anymore. The increase of the design stresses in the girder are largely compensated by the higher yield resistance of steel S690. On the other hand, local buckling of the web becomes an issue, with class 4 cross-sections.

The verification regarding flange induced buckling must be adapted by considering the non-symmetry of the composite section. It is also necessary to account for the actual design stresses in the flanges, because the value of the yield resistance of S690 would be too conservative.

The justification against LTB of the compression flange is also improved, by using the general check method which considers the reserve in resistance at

ULS. The cross-girders used in the bracing frames remain identical, and the vertical stiffeners are smaller.

Fatigue issues become the decisive criterion in the design B. With the increase of the stresses in the flanges, the detail of the transverse weld of the vertical T-shaped stiffener web on the lower flange at mid-span is critical. It limits the reduction of the cross-section area of the girders, more specifically the lower flange, and would require a treatment to improve its FAT category.

7.2. Analysis of the design C

The weight of the girders in the design C also decreases consequently compared to the design A. It is very close to the steel weight of the design B.

The design stresses at ULS are higher in the extreme fibres of the tubular flanges. Nevertheless, the average stresses in the flanges remain low because the mid-plane of the tube is higher in the section. Besides, the tubes are in class 1 at support; a partial plastification of the tubes could still be used.

The justification against LTB of the compression flange is improved, thanks to the resistance of the tubular flanges against torsion. The cross-girders can be lighter, although the vertical stiffeners are even smaller than in the design B.

The local buckling of the web is improved because of the fixed connections between the web and the flanges. This enhances the limit between cross-sections classes 3 and 4 and the design shear buckling resistance.

Fatigue issues remain the decisive criterion in the design C. The detail of the transverse weld of the vertical T-shaped stiffener web on the lower flange at mid-span is still critical; the detail is higher in the cross-section, but the design stresses increase.

Last but not least, some problems related to the construction of the bridge appear. The welds between the vertical stiffeners and the tubular flanges are more difficult to carry out; and the new detail of the butt weld of the lower flange to the vertical plate at support has to be executed. Finally, the length of the tubes is limited in stock for the required diameter and thicknesses, which means more butt welding to assemble the tubular flanges.

8. Notation

E_a	Young's modulus for steel
f_{yk}	Yield strength of the structural steel
h_w	Height of the web
I_p	Second moment of area of the stiffener
I_T	St. Venant torsional constant of the stiffener
I_w	Stiffener's warping cross-section constant
k_σ	Plate buckling coefficient for normal stresses
k_τ	Plate buckling coefficient for shear stresses
m	Working coefficient in the flanges
M_{Ed}	Design bending moment
$M_{f,Rd}$	Plastic moment resistance without the web
$M_{pl,Rd}$	Plastic moment resistance
t_w	Thickness of the web
$V_{b,Rd}$	Design shear buckling resistance
V_{cr}	Critical shear resistance
V_σ	Post-buckled shear strength
V_{Ed}	Design shear force
$V_{pl,a,Rd}$	Design plastic shear resistance
V_{Rd}	Design shear resistance
α	Aspect ratio of a web panel
$\alpha_{ult,k}$	Factor for the characteristic elastic resistance
$\alpha_{cr,op}$	Factor for the LTB critical elastic resistance
γ_{Mf}	Partial factor for the detail fatigue strength
γ_{Ff}	Partial factor for the stress range $\Delta\sigma_{E,2}$
ε	Factor for determining the cross-section class
λ	Damage equivalent factor
$\bar{\lambda}_p$	Winter's coefficient
ψ	Stress ratio
Φ	Damage equivalent impact factor
$\overline{\eta}_1$	Working coefficient (bending at $h_w/2$)
$\overline{\eta}_3$	Working coefficient (shear at $h_w/2$)
$\sigma_{cr,D}$	Critical lateral-torsional buckling stress
σ_{Dv}	Uniform component of $\sigma_{cr,D}$
σ_{Dw}	Non-uniform component of $\sigma_{cr,D}$
σ_D	Lateral-torsional buckling stress
σ_{Ed}	Design stress
$\sigma_{act,Ed}$	Actual stress in the stiffener
$\Delta\sigma_{E,2}$	Equivalent constant amplitude stress range
$\Delta\sigma_c$	Reference value for the fatigue strength
$\Delta\sigma_{fat}$	Stress variation obtained with the FLM3
τ_{cr}	Elastic critical shear buckling stress
χ_{op}	Global reduction factor

9. References

[1] *Eurocode 3: Design of steel structures - Part 1-1: General rules and rules for buildings*, Comité européen de normalisation CEN. Bruxelles, 2005.

[2] *Eurocode - Basis of structural design. Annex A2*, Comité européen de normalisation CEN. Bruxelles, 2005.

[3] SETRA, *Guidance book, Eurocodes 3 et 4, Application to steel-concrete composite road bridges*. Bagneux: Service d'études techniques des routes et autoroutes, 2010.

[4] *Eurocode 4 - Design of composite steel and concrete structures - Part 2: General rules and rules for bridges*, Comité européen de normalisation CEN. Bruxelles, 2005.

[5] U. Kuhlmann, L. Davaine, B. Braun, and others, *Design of Plated Structures: Eurocode 3: Design of Steel Structures, Part 1-5: Design of Plated Structures*. John Wiley & Sons, 2012.

[6] J.-P. Lebet and M. A. Hirt, *Ponts en acier : Conception et dimensionnement des ponts métalliques et mixtes acier-béton : Traité de Génie Civil 12*. Lausanne: Presses polytechniques et universitaires romandes, 2009.

[7] *Eurocode 3 - Design of steel structures - Part 2: Steel Bridges*, Comité européen de normalisation CEN. Bruxelles, 2006.

[8] *Eurocode 3 - Design of steel structures - Part 1-5: Plated structural elements*, Comité européen de normalisation CEN. Bruxelles, 2006.